Memoirs of the Scientific Sections of the Romanian Academy
Tome XXXV, 2012

CHEMISTRY

2D IR CORRELATION SPECTROSCOPY IN WOOD SCIENCE

CARMEN-MIHAELA POPESCU [1,2]✉, MARIA-CRISTINA POPESCU [2] and BOGDAN C. SIMIONESCU[1,2], member of the Romanian Academy

[1] *"Gheorghe Asachi" Technical University of Iasi, Department of Natural and Synthetic Polymers, Iasi, Romania*
[2] *"Petru Poni" Institute of Macromolecular Chemistry of Romanian Academy, Iasi, Romania*

Generalized 2D correlation spectroscopy is a well-established technique that provides considerable utility and benefit in various spectroscopic studies of polymers. Some of the important features of generalized 2D correlation spectra are simplification of complex spectra consisting of many overlapped peaks, enhancement of spectral resolution by spreading peaks along the second dimension, unambiguous assignments through the correlation of bands selectively coupled by various interaction mechanisms, and determination of the sequence of the spectral peak emergence.

Key words: 2D correlation, vibrational spectroscopy, wood, degradation.

1. INTRODUCTION

Two dimensional (2D) correlation spectroscopy was applied first of all in NMR spectroscopy. In the field of NMR, 2D correlation spectroscopy is obtained by using double Fourier transformation for a set of time domain data collected in the relaxation of nuclei under multiple-pulse excitation. The last 20 years this analytical method was applied also to vibrational spectroscopy. The reason lies on the difference between the time scales of relaxation of spin and vibration. The relaxation time of molecular vibration (picosecond range) is many orders of magnitude shorter than the typical spin relaxation time (microsecond range or even longer). The ordinary spectrometer cannot excite molecular vibration and detect its relaxation signal in such a short time. Thus, 2D correlation spectroscopy cannot be obtained for molecular vibrational spectroscopy as it is obtained for NMR by using multiple-pulse excitation [20].

✉ 41A, Grigore Ghica Voda Alley, 700487 Iasi, Romania. E-mail: mihapop@icmpp.ro
Second author (SA) e-mail: cpopescu@icmpp.ro. Third author (TA) e-mail: bcsimion@icmpp.ro

The first 2D vibrational correlation spectra were obtained in experiments with IR spectroscopy, when mechanical perturbations were added to the samples and IR vibrational spectra associated with perturbations were probed in the relaxation. Since the relaxation time caused by perturbation is much shorter than that of molecular vibration, the signals in the relaxation process can be easily measured with a conventional spectrometer by using time resolved technique. Based on it, 2D infrared correlation spectra were introduced and gained an increasing importance. The early attempts at 2D correlation spectroscopy were heavily influenced by the approaches in NMR, where only time-dependent changes in spectral signals are considered.

The concept of generalized 2D correlation spectroscopy was proposed in 1993, in a more general application form [21]. Generalized 2D correlation spectroscopy is the extension of theory of 2D correlation spectroscopy, which was mainly reflected in two facets. First, it is the extension of perturbation modes. The perturbations are not limited to those varying sinusoidally and can vary arbitrarily. Furthermore, any physical or chemical variables, such as optical, magnetic and thermal perturbations or pressure, concentration, and pH value can be considered as perturbations. Secondly, generalized 2D correlation spectroscopy is the extension of other types of spectroscopy, such as Raman, X-ray, ultraviolet, fluorescence and infrared ones. Generalized 2D correlation analysis can be also developed between different types of spectroscopy [21, 23].

2. THE GENERALIZED TWO-DIMENSIONAL CORRELATION SPECTROSCOPY

2D correlation spectroscopy is obtained by extracting the information contained in the spectra in two dimensions, which is the function of two dependent spectral variables. The basic concept used to build a 2D correlation spectrum is the analysis of dynamic spectrum, *i.e*., the spectral analysis in the frequency domain of the spectral characteristics that change in the time domain due to external perturbations. These perturbations may be of diverse nature, i.e. temperature [12, 31, 35, 45], pressure [42], concentration [36, 37], pH [19, 47] or others.

The 2D correlation spectroscopy comprises, basically, two types of correlation spectra, the synchronous ($\Phi(\nu_1, \nu_2)$) and asynchronous ($\Psi(\nu_1, \nu_2)$) ones.

In order to apply 2D correlation spectroscopy, the dynamic spectra must be first calculated. Considering a time-dependent fluctuation of the spectral intensity $y(\nu, t)$ observed for a period of time between T_1 and T_2, the dynamic spectrum is defined as

$$\tilde{y}(\nu,t)=\begin{cases} y(\nu,t)-\overline{y}(\nu) & T_1 \le t \le T_2 \\ 0 & others \end{cases}$$

where $\overline{y}(\nu)$ is the reference spectrum.

The reference spectrum can be arbitrarily selected, but usually it is set as a time-averaged spectrum. Then, the dynamic spectrum measured in the time domain has to be converted through the Fourier transform into the frequency domain according to

$$\tilde{Y}_1(\omega)=\int_{-\infty}^{+\infty}\tilde{y}(\nu_1,t)e^{-i\omega t}dt=\tilde{Y}_1^{\mathrm{Re}}(\omega)+i\tilde{Y}_1^{\mathrm{Im}}(\omega)$$

where $\tilde{Y}_1^{\mathrm{Re}}(\omega)$ and $\tilde{Y}_1^{\mathrm{Im}}(\omega)$ are the real and imaginary components of the Fourier transform of signal $\tilde{y}(\nu_1,t)$. Fourier frequency ω represents the frequency component of the time-dependent variation of the signal. Similarly, the conjugate of Fourier transform of dynamic spectra is

$$\tilde{Y}_2^{*}(\omega)=\int_{-\infty}^{+\infty}\tilde{y}(\nu_2,t)e^{i\omega t}dt=\tilde{Y}_2^{\mathrm{Re}}(\omega)-i\tilde{Y}_2^{\mathrm{Im}}(\omega)$$

The 2D correlation intensity between the $\tilde{y}(\nu_1,t)$ and $\tilde{y}(\nu_2,t)$ signals can be calculated using the equation

$$X(\nu_1,\nu_2)=\frac{1}{\pi(T_2-T_1)}\int_0^{\infty}\tilde{Y}_1(\omega)\cdot\tilde{Y}_2^{*}(\omega)d\omega=\Phi(\nu_1,\nu_2)+i\Psi(\nu_1,\nu_2)$$

where the real and imaginary components of $X(\nu_1, \nu_2)$, $\Phi(\nu_1, \nu_2)$ and $\Psi(\nu_1, \nu_2)$ are the synchronous and asynchronous correlation spectral intensities generated from the corresponding dynamic spectra.

The time variable can be replaced by other physical or chemical variables. This 2D correlation spectroscopy calculation method through Fourier transform is complex, especially if there are a large number of dynamic spectra. In this case, the Fourier transform of the signal will be a huge load for the calculation.

Another method, more frequently used in the calculation of 2D correlation spectroscopy, is the Hilbert transform method, which is more simple and efficient than Fourier transform method, and also offers a specific physical meaning.

Using the Hilbert transform method, and if the discrete set of data is represented in term of a matrix, the synchronous spectrum can be obtained through the dot product of a mean-centered spectral matrix of the dynamic spectrum vector $\tilde{y}(\nu)$

$$\Phi(\nu_1,\nu_2)=\frac{1}{m-1}\cdot\tilde{y}(\nu_1)^T\cdot\tilde{y}(\nu_2)$$

The corresponding asynchronous correlation spectra can be calculated according to

$$\Psi(\nu_1,\nu_2)=\frac{1}{n-1}\cdot\tilde{y}(\nu_1)^T\cdot N\cdot\tilde{y}(\nu_2)$$

where N is the Hilbert–Noda matrix [22].

$$N_{kj}=\begin{cases}0 & if \quad j=k\\ \dfrac{1}{\pi(k-j)} & otherwise\end{cases}$$

Basically the synchronous spectrum contains information on the in phase changes that occur while the asynchronous spectrum supplies information about spectral variances that are out-phased. A synchronous spectrum displays overall variance of the data and can easily sort out non-overlapped bands. However, if the bands overlap, the asynchronous spectrum is of greater value to analyze complex 1D spectra of different systems.

3. DATA SIMULATION

One of the major obstacles to the widespread use of 2D correlation technique is the apparent difficulty in the interpretation of the complex features appearing on 2D spectral maps.

In the case of extensive band overlapping, certain misleading results could be generated from the 2D correlation map by evidencing a wrong number of auto- and cross-peaks. Many researchers use data pre-treatment for the proper working of 2D correlation analysis in order to solve the peak overlap problem. Interpretation of 2D spectra can be greatly assisted by the use of simulated data with some known dynamic patterns [32], too. Generally, the contours of the IR spectral bands have Gaussian shape types. The equation which describes these types of contour is

$$y=y_c e^{-2\frac{(x-x_c)^2}{w^2}}$$

where y_c is the maximum value of the function (band intensity), x_c is the value on the x axis corresponding to y_c (band position), w is band width.

The band intensity, position and width can be modified by external perturbations. These modifications can be evidenced by plotting 2D correlation spectra of Gauss functions. For data simulation an isolated single band, with the y_c=1 a.u., x_c= 1500 cm^{-1} and w=200 cm^{-1} parameters was used.

If as a result of the external perturbation the band position is linearly shifted along the spectral axis to higher wavenumbers from 1500 cm^{-1} to 1550 cm^{-1}, the synchronous spectrum shows the characteristic four-way symmetric "***four-leaf-clever***" cluster pattern, comprising two auto-peaks at 1450 and 1600 cm^{-1} and two negative cross-peaks at Φ(1600, 1450) cm^{-1} and Φ(1450, 1600) cm^{-1}. The center of the cluster is located near the spectral coordinate corresponding to the peak maximum position of the average spectrum. The asynchronous spectrum shows the characteristic pattern known as the "***butterfly***" pattern. The cluster consists of a pair of elongated cross-peaks of opposed signs located very close to the diagonal line of the 2D spectrum. This butterfly pattern is a very distinct and easily recognized indicator for the existence of a shift in the band position. If the elongated cross-peak above the diagonal line is negative and that below the diagonal line is positive, the band position is shifted to higher wavenumbers. Opposite signs of the cross-peaks indicate the opposite direction of band shifts.

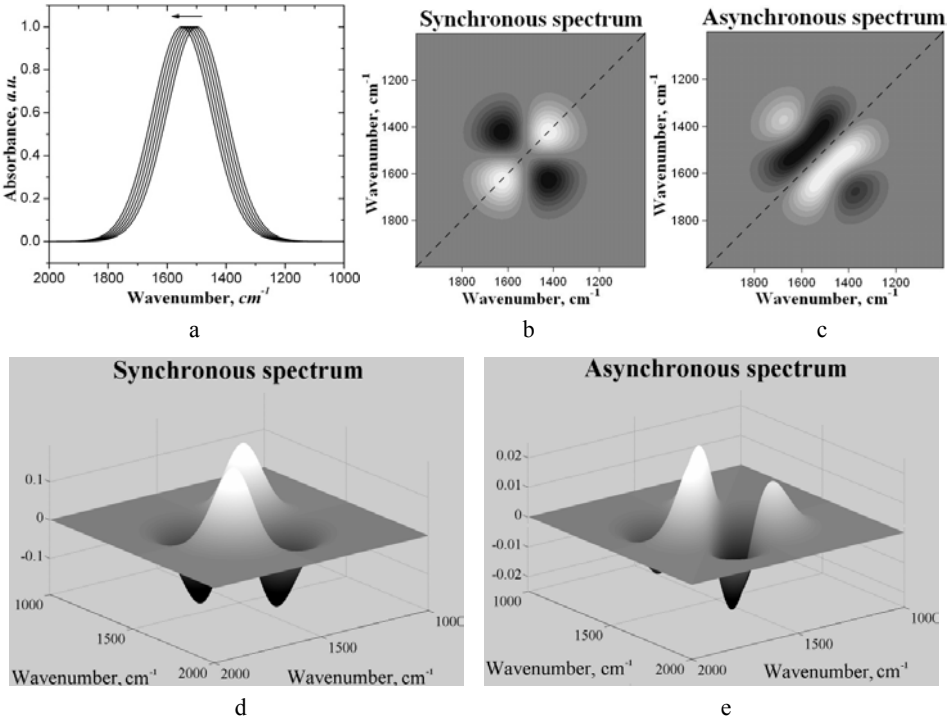

Fig. 1. Simulated models for a band position shifts to the higher wavenumber direction: Gauss contour (a) and corresponding synchronous (b, d) and asynchronous spectra (c, e).

When as a result of the external perturbation the width of the band linearly varies from 200 cm^{-1} to 250 cm^{-1} (Fig. 2a), the synchronous spectrum shows a four-way symmetric "***four-leaf-clever***" cluster pattern, too. The auto-peaks are located at 1400 and 1600 cm^{-1} and two positive cross-peaks at Φ(1600, 1400) cm^{-1} and Φ(1400, 1600) cm^{-1} can be observed. The asynchronous spectrum shows the eight-way cross-like cluster pattern, comprising four positive and four negative cross-peaks. This pattern looks like a "***moon flower***". As in the previous case, if the width of the band decreases the sign of the cross-peaks in the asynchronous spectrum has an opposite sign.

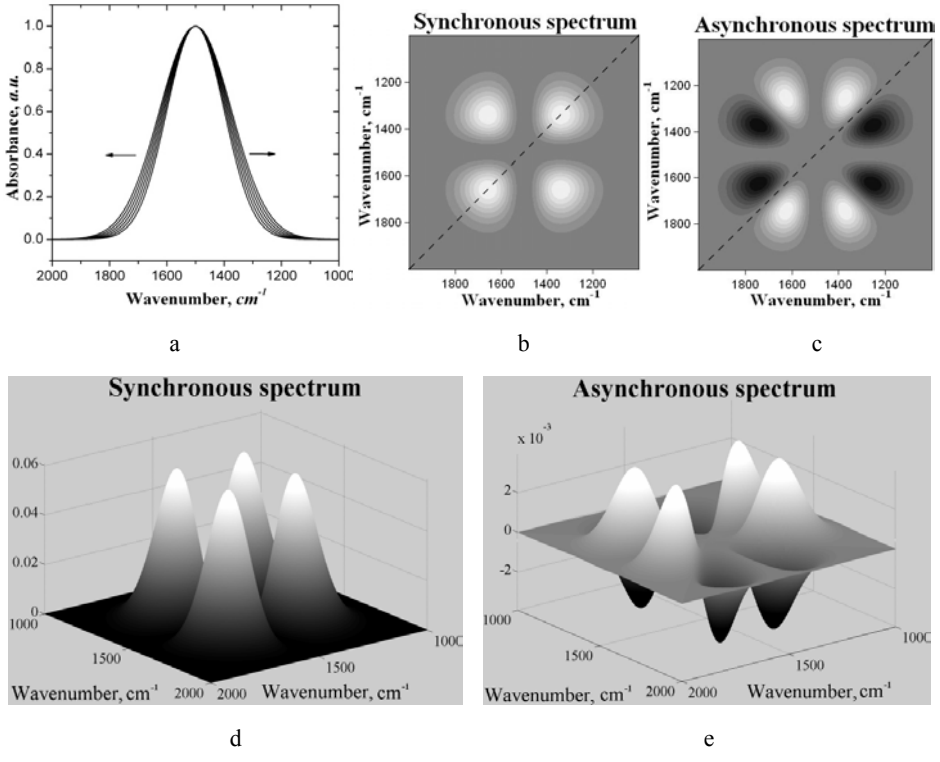

Fig. 2. Simulated models for a band width shifts: Gauss contour (a) and corresponding synchronous (b, d) and asynchronous spectra (c, e).

In most cases, more than one parameter is influenced by the external perturbation. Another situation considered is the one in which the peak height increases linearly from 1 to 1.25 a.u. and the band width increases from 200 to 250 cm^{-1}. The synchronous spectrum shows a symmetric pattern, consisting of two auto-peaks and two positive cross-peaks. These peaks are overlapped, but an empty space is

formed between them. The asynchronous spectrum consists in four positive cross-peaks and four negative cross-peaks. In this case, the pattern resembles a "***moon flower***", too. The difference consists in the fact that the petals of the flower are coupled two by two. The same synchronous and asynchronous spectra are obtained when the peak height and width decrease.

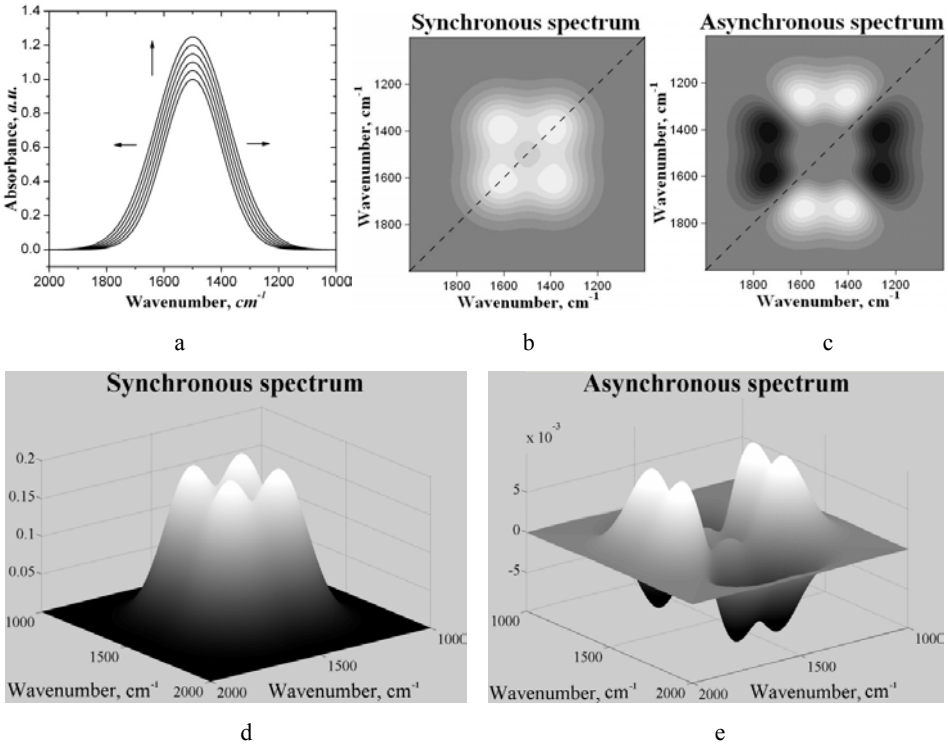

Fig. 3. Simulated models for a band width and height increasing: Gauss contour (a) and corresponding synchronous (b, d) and asynchronous spectra (c, e).

The pattern of synchronous and asynchronous spectra changes when the band width decreases from 200 to 150 cm^{-1}. In this case the synchronous spectrum shows a characteristic four-way cluster pattern, consisting in a dominant central auto-peak surrounded by two less intense auto-peaks and four negative cross-peaks. The asynchronous spectrum shows the four-way symmetric cross-like cluster pattern, containing two positive and two negative cross-peaks. The symmetry axes of the 2D peaks clusters are aligned with the spectral axes of the 2D correlation spectra, and thus the pairs are formed between the cross-peaks in either vertical or horizontal direction.

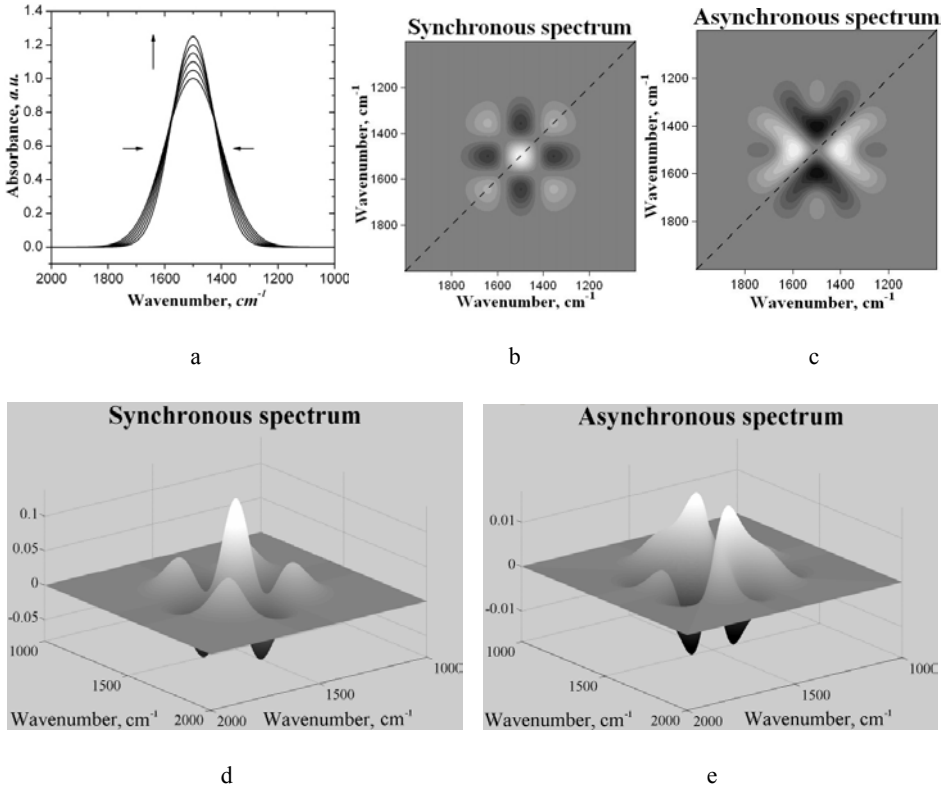

Fig. 4. Simulated models for a band width decreasing and height increasing: Gauss contour (a) and corresponding synchronous (b, d) and asynchronous spectra (c, e).

If as a result of an external perturbation the peak height linearly increases from 1 to 1.25 a.u. and band position shifts from 1500 to 1550 cm^{-1}, the cluster pattern in the synchronous spectrum is no longer four-way symmetric, and one auto-peak becomes disproportionately large as compared to the other. Such a pattern is sometimes referred to as the "***angel***" pattern with cross-peak wings. The asynchronous spectrum are also distorted from the standard butterfly pattern. The elongated asynchronous cross-peaks near the diagonal are now distributed closer to the stronger auto-peak side. The pair of the main cross-peaks looks almost as they would represent two distinct bands. This case can be easily confused with the two overlapped bands. If the band position is shifted to lower wavenumbers and band intensity increases, the synchronous and asynchronous spectra represent reverse images in respect to the secondary diagonal line. In addition, the sign of the cross-peaks in asynchronous spectra are inverted.

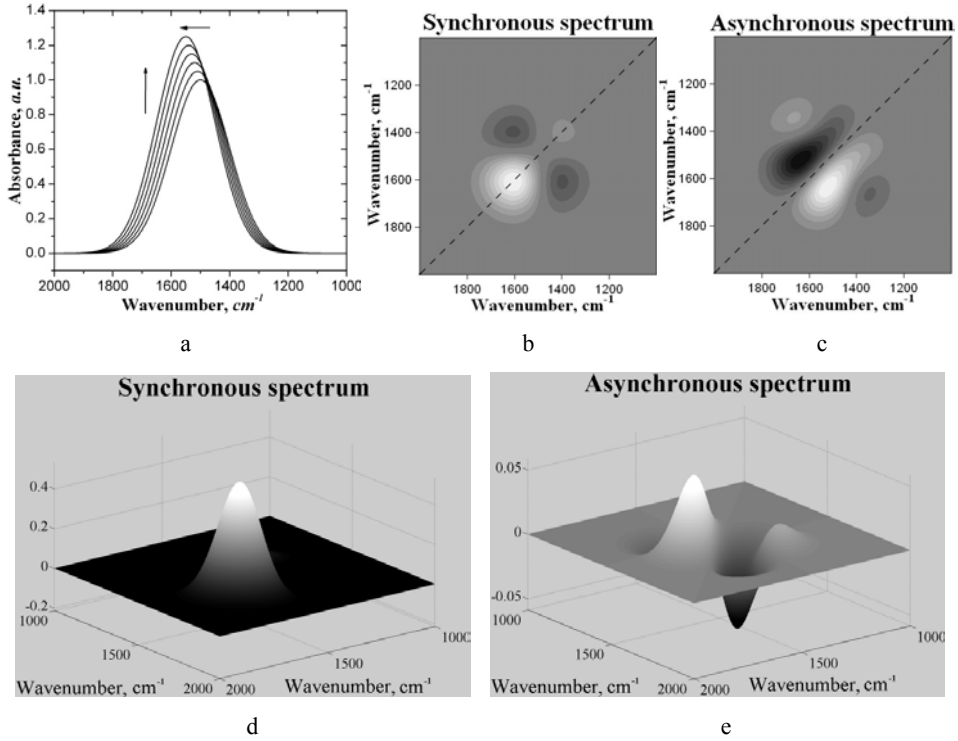

Fig. 5. Simulated models for a band position shift to higher wavenumbers and height increasing: Gauss contour (a) and corresponding synchronous (b, d) and asynchronous spectra (c, e).

The presence of multiple correlation peaks in about all asynchronous spectra may give an erroneous impression that there may be multiple hidden bands involved in the formation of such clusters. In reality, only a single band is involved. Whenever such a pattern is observed, one may assume that there is a possibility of a single band shift.

The models of synchronous and asynchronous spectra are very useful to assess the modifications appearing in the infrared spectra of complex materials or following the action of different external perturbations, by comparing the 2D correlation spectra with these models.

4. 2D IR CORRELATION SPECTROSCOPY IN WOOD CHARACTERIZATION

Due to its unique and useful properties, wood has remained an important substance throughout history. It is recyclable, renewable, and biodegradable. Many species are shock resistant, bendable, and stable (although all wood changes dimensions as it loses or gains moisture). Wood can be treated to resist decay, and with proper construction techniques and stains or paint wood buildings can last

hundreds of years. Today, wood is used in tools, paper, buildings, bridges, guardrails, railroad ties, posts, poles, mulches, furniture, packaging, and thousands of other products [1, 46].

However, wood is a complex material formed mainly of three components – cellulose, lignin and hemicelluloses. In addition to these polymeric components, wood may contain extractives in more or less large amounts including several classes of organic compounds like sugars, flavonoids, tannins, terpenes, fats or waxes [8].

The main components of woody cell walls are degraded to different extents by various groups of organisms. Both the so-called soft rot and brown rot fungi, belonging to the *Ascomycetes* and *Basidiomycetes*, respectively, decompose mainly the polysaccharides. A third group, also *Basidiomycetes* and known as white rot fungi, attacks both lignin and polysaccharides either simultaneously or successively.

Wood is also a good light absorber. Among the constituent polymers, lignin is an excellent light absorber leading to the formation of free radicals. These ones react with oxygen to produce chromophoric carbonyl and carboxyl groups, which are responsible for color changes [3, 8].

The characterization of wood is a complex procedure involving several steps wherein wood components are isolated or degraded to monomeric fragments. These procedures destroy the wood matrix and require large sample sizes and long analysis time [4]. Fourier transformed infrared (FT-IR) spectroscopy has been used as a simple technique for obtaining rapid information on the structure of wood constituents and chemical changes taking place in wood due to various degradations/ modifications. Contrary to conventional chemical analysis, this technique requires small sample sizes and short analysis time [2]. Even if it is a rapid technique it still has some disadvantages when very small differences do exist between the samples or when a correlation between different degradation factors and wood structure is required to be establish. For this, a powerful, rapid and new very sensitive method can be used. Usually, the 2D correlation IR spectroscopy enhances the spectral resolution and yields new information – not acquired through conventional IR and its derivative spectra.

This method was used for different types of samples and for natural polymers, too. To give only a few examples, Popescu *et al*. [33, 34, 36], Pi *et al*. [25] and Watanabe *et al*. [45] studied specific interactions in polymers and polymer blends, Shinzawa *et al*. [40] studied finely ground microcrystalline cellulose, Labbé *et al*. [15] analyzed pine wood with varying amount of cellulose contents, Watanabe *et al*. [44] studied the transition of cellulose crystals, Huang *et al*. [9] studied bamboo fibers. Popescu *et al*. [26, 27] used 2D IR to compare eucalyptus wood chips, brown stock pulp, and chlorite-bleached pulp samples, and to evaluate the degradation stages in naturally aged lime wood. Stevanic *et al*. [43] used dynamic 2D IR to study interactions of wood polymers such as cellulose, lignin, protein, pectin and

xyloglucan. Li *et al*. studied ginseng from different regions [17, 18, 48], while Hinterstoisser *et al*. [6] and Hishikawa *et al*. [7] used this method for cellulose characterization.

Huang *et al*. [11] evaluated the differences between three hard to distinguish wood species (*Dalbergia odorifera* T. Chen, *Pterocarpus santalinus* L.F. and *Pterocarpus soyauxii*). They established the existing differences by using Fourier transform infrared spectroscopy (FT-IR), second derivative IR spectra and two-dimensional infrared (2D-IR) correlation spectroscopy. The differences between woods were clearly seen in the 2D correlation spectra. The authors combined the information of bands in FT-IR spectra and auto-peaks in 2D IR spectra. In the 1300–1800 cm^{-1} region, *D. odorifera* has five auto-peaks, *P. santalinus* four auto-peaks, while *P. soyauxii* has only two auto-peaks. This comparative method can clearly reveal the differences of categories and amounts of chemical constituents in different woods. At the same time, Huang *et al*. [10] identified the poplar and Eucalyptus through the Fourier transform infrared spectroscopy (FT-IR) combined with two-dimensional correlation spectroscopy (2D IR).

Two-dimensional IR correlation spectroscopy can be also used to evaluate the chemical changes occuring when wood is subjected to different degradation factors, such as soft rot fungi or/and UV light, temperature and humidity. To identify and evaluate the occuring chemical changes, 2D IR correlation spectra generated from the exposure time dependent infrared spectra of the soft rot decayed wood and photodegraded wood were obtained. The correlation spectra clearly show the presence of synchronous and asynchronous correlation peaks among different modes of molecular vibrations. In practice, when 2D IR correlation analyses are performed it is usually more convenient to scan only a part of the correlation map to pick up a useful local feature of the correlation intensity profile rather than displaying the entire spectral region.

Biodegradation of lime wood with *Trichoderma viride*

Lime wood sheets were exposed to *T. viride* fungus for periods up to 84 days. The average mass loss of wood samples at the end of the exposure was 14.3 wt%. The fungus action induced a continuous decrease of sample mass, of 0.05 wt %/day during the first 34–35 days, and was five times faster (0.24 wt%/day) in the next period of 50 days.

FT-IR spectroscopy combined with 2D IR correlation spectroscopy allowed the evaluation of the qualitative and quantitative changes in carbohydrate components in wood decayed by soft-rots, providing detailed information about the modifications induced by fungi decay. In 2D IR correlation spectra, the most important differences were observed in the 1800–1195 cm^{-1} region and these were evaluated for two time intervals, of 0–35 days and 35–84 days (taking in account the different slopes of the mass loss curves) [28].

In the synchronous 2D IR correlation spectrum of the exposure time range (0–35 days) (Fig. 6a), six auto-peaks at $\Phi(1728, 1728) > 0$, $\Phi(1641, 1641) > 0$, $\Phi(1460, 1460) > 0$, $\Phi(1427, 1427) > 0$, $\Phi(1375, 1375) > 0$ and $\Phi(1255, 1255) > 0$ and the corresponding positive cross-peaks were observed, implying that the bands at 1728, 1641, 1460, 1427, 1375 and 1255 cm^{-1} show changes during exposure time.

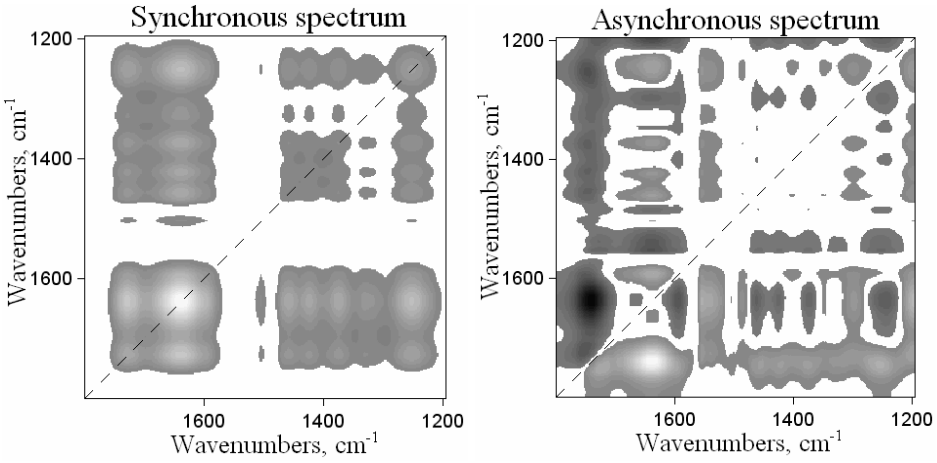

Fig. 6. Synchronous (a) and asynchronous (b) 2D-correlation spectra in the 1800–1195 cm^{-1} region issued from the exposure time-dependent IR spectra. Biodegradation with *T. viride*, time range of 0–35 days.

The asynchronous 2D IR correlation spectrum resulting from the exposure time-dependent IR spectral variations in the time range of 0–35 days (Fig. 6b) shows ten bands at 1741, 1725, 1641, 1597, 1554, 1460, 1427, 1379, 1350 and 1255 cm^{-1}. Positive cross-peaks at $\Psi(1641, 1597) > 0$, $\Psi(1641, 1462) > 0$, $\Psi(1641, 1427) > 0$, $\Psi(1641, 1379) > 0$, $\Psi(1641, 1255) > 0$, $\Psi(1554, 1460) > 0$, $\Psi(1554, 1427) > 0$, $\Psi(1554, 1375) > 0$, $\Psi(1554, 1255) > 0$, $\Psi(1350, 1255) > 0$, and negative cross-peaks at $\Psi(1741, 1725) < 0$, $\Psi(1741, 1641) < 0$, $\Psi(1741, 1554) < 0$, $\Psi(1741, 1460) < 0$, $\Psi(1741, 1427) < 0$, $\Psi(1741, 1379) < 0$, $\Psi(1741, 1255) < 0$, $\Psi(1641, 1554) < 0$, were identified. Based on the fundamental rule of an asynchronous spectrum, the spectral intensity change at 1641 cm^{-1} occurs before those at 1741, 1725, 1597, 1554, 1460, 1427, 1379, 1350 and 1255 cm^{-1}.

Thus, the following sequence of spectral intensity changes was obtained:

$$1640 > 1255, 1350 > 1375 > 1427 > 1460 > 1597 > 1554 > 1725 > 1741\ cm^{-1}$$

This sequence means that the moment of absorbed O–H is changing first, followed by the C–O linkages in hemicelluloses (xyloglucan) and C–H linkages in

cellulose and hemicelluloses and then by C=O linkages in non-conjugated ketones, carboxyl groups and acetyl groups in hemicelluloses (xyloglucan) and C=O linkages of various groups from carbohydrates.

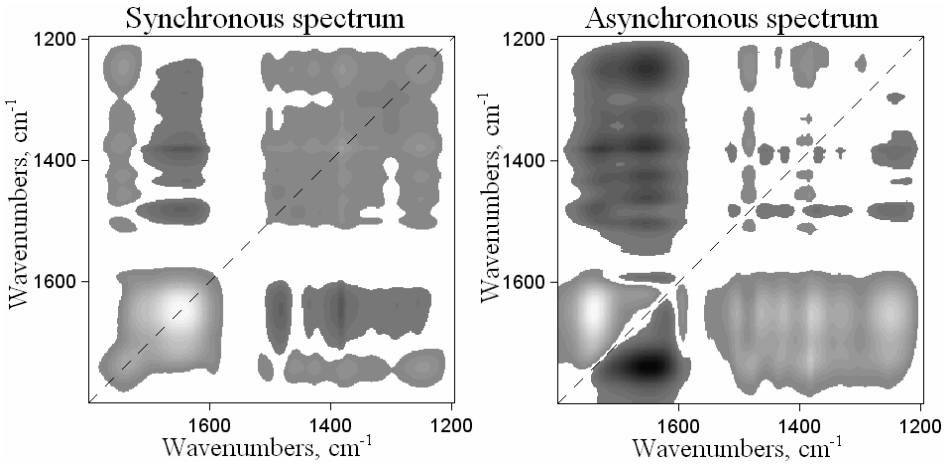

Fig. 7. Synchronous (a) and asynchronous (b) 2D correlation spectra in the 1800–1195 cm^{-1} region issued from the exposure time-dependent IR spectra.
Biodegradation with *T. viride*, time range of 35–84 days.

In the synchronous 2D IR correlation spectrum of the second exposure time range of 35–84 days (Fig. 7a), seven auto-peaks at $\Phi(1745, 1745) > 0$, $\Phi(1649, 1649) > 0$, $\Phi(1481, 1481) > 0$, $\Phi(1462, 1462) > 0$, $\Phi(1427, 1427) > 0$, $\Phi(1381, 1381) > 0$ and $\Phi(1251, 1251) > 0$ and the corresponding positive and negative cross-peaks were observed, implying that the bands at 1745, 1649, 1481, 1462, 1427, 1381 and 1251 cm^{-1} show changes during this exposure time.

The asynchronous 2D IR correlation spectrum (Fig. 7b) shows ten bands at 1745, 1725, 1649, 1597, 1481, 1462, 1427, 1381, 1334 and 1251 cm^{-1}. Positive cross-peaks at $\Psi(1745, 1649) > 0$, $\Psi(1745, 1597) > 0$, $\Psi(1481, 1462) > 0$, $\Psi(1481, 1427) > 0$, $\Psi(1481, 1381) > 0$, $\Psi(1481, 1334) > 0$, $\Psi(1481, 1251) > 0$, $\Psi(1427, 1251) > 0$, $\Psi(1381, 1334) > 0$, $\Psi(1381, 1251) > 0$, $\Psi(1334, 1251) > 0$ and negative cross-peaks at $\Psi(1745, 1462) < 0$, $\Psi(1745, 1427) < 0$, $\Psi(1745, 1381) < 0$, $\Psi(1745, 1334) < 0$, $\Psi(1745, 1251) < 0$, $\Psi(1649, 1597) < 0$, $\Psi(1649, 1462) < 0$, $\Psi(1649, 1427) < 0$, $\Psi(1649, 1381) < 0$, $\Psi(1649, 1334) < 0$, $\Psi(1649, 1251) < 0$, $\Psi(1462, 1381) < 0$, $\Psi(1427, 1381) < 0$ were identified. Based on the fundamental rule of an asynchronous spectrum, the following sequence of spectral intensity changes was obtained:

$$1649 > 1481 > 1381 > 1334 > 1427, 1462 > 1597 > 1251 > 1725 > 1741 > 1597\ cm^{-1}$$

This sequence means that the moment of absorbed O–H is changing first, followed by the C–H linkages in cellulose and hemicelluloses and then by the C–O linkages of acetyl groups in hemicelluloses, C=O linkages in non-conjugated ketones, carboxyl groups and acetyl groups in hemicelluloses (xyloglucan) and then by the C=O bonds of various groups from carbohydrates. It is known that *T. viride* is removing only carbohydrates, so that the modification of these bands results only from hemicelluloses and cellulose removal.

Following the interpretation of the 2D correlation spectra, the results show that the formation of oxidized structures takes place at the beginning of the biodegradation process. This is evidenced by the variation of the intensity of the bands assigned to C=O vibrations in cellulose and hemicelluloses. After 35 days of exposure to fungi, the oxidation products are yielded with a higher rate due to the weakened structure of the wood. *T. viride* fungus is a producer of a cellulolytic enzyme system which forms a synergistic complex of endoglucanases (endo-1,4-β-glucanases), hydrolyzing internal bonds and opening free chain ends for cellobiohydrolases (exo-1,4-β-glucanases) to cleave off cellobiose units (reducing and non-reducing ends), which are then broken down to glucose by β-glucosidase [24]. The endo-β-glucanases and cellobiohydrolases synergistically hydrolyze cellulose into smaller cellooligosaccharides, mainly cellobiose, whereas β-glucosidase hydrolyzes aryl- and alkyl-glucosides, cellobiose and cellodextrins.

At the same time, the hemicelluloses xylan backbone is degraded by the ectoenzyme endo-1,4-β-xylanase within the xylose chain (endohydrolysis) to xylo-oligomers, xylobiose and xylose. Intracellular and/or membrane-bound xylan 1,4-β-xylosidase removes successively D-xylose residues from the non-reducing chain ends of small oligosaccharides.

The side groups are splited by some accessory enzymes, such as xylan α-1,2-glucuronidase that hydrolyzes the α-D-1,2-(4-O-methyl)glucuronosyl links, α-arabinosidase that attacks the arabinose side groups in arabinoxylans, while acetylesterase removes the acetyl groups [39]. The molecules are first degraded by ectoenzymes (extracellular enzymes) into smaller fragments, which are then metabolized by intracellular enzymes to energy and fungal biomass. Independently, the exoenzymes attack the end of the macromolecular substrate, while the endoenzymes splits within the molecule. Finally, small molecules or fragments containing carboxyl, hydroxyl or carbonyl groups are formed, these ones being lost or remaining in wood structure.

Biodegradation of lime wood with *Chaetomium globosum*

Lime wood sheets were exposed to *C. globosum* fungus for a period up to 133 days. The fungus action was observed through the continuous decrease of sample mass, of 0.49 wt%/day in the first 70 days and of 0.29 wt%/day in the next period of 63 days. The average mass loss of lime wood blocks after 133 days of exposure to *C. globosum* was of 50.4%.

Exposure time-dependent IR spectra of biodegraded lime wood combined with 2D correlation analysis and their second derivative analysis can provide detailed information on the modifications induced by fungus decay [29]. 2D correlation spectra provided the possibility to explore the structural changes in wood due to a variety of oxidoreductions, some of which resulting in the cleavage of the polysaccharide chain, and demethoxylation of lignin.

2D IR correlation spectra generated from the exposure time-dependent infrared spectra of the *C. globosum* decayed lime wood were obtained in the 1850 – 1195 cm^{-1} region for two time domains of 0–70 days, and 70–133 days, respectively (taking into account the different slope of the mass loss curve) [29]. Correlation spectra, in this region, clearly show the presence of synchronous and asynchronous correlation peaks among different modes of molecular vibrations.

In the synchronous 2D correlation IR spectrum of the exposure time range of 0–70 days (Fig. 8a), seven auto-peaks at $\Phi(1738, 1738) > 0$, $\Phi(1674, 1674) > 0$, $\Phi(1618, 1618) > 0$, $\Phi(1575, 1575) > 0$, $\Phi(1373, 1373) > 0$, $\Phi(1327, 1327) > 0$ and $\Phi(1246, 1246) > 0$ and the corresponding positive and negative cross-peaks were identified.

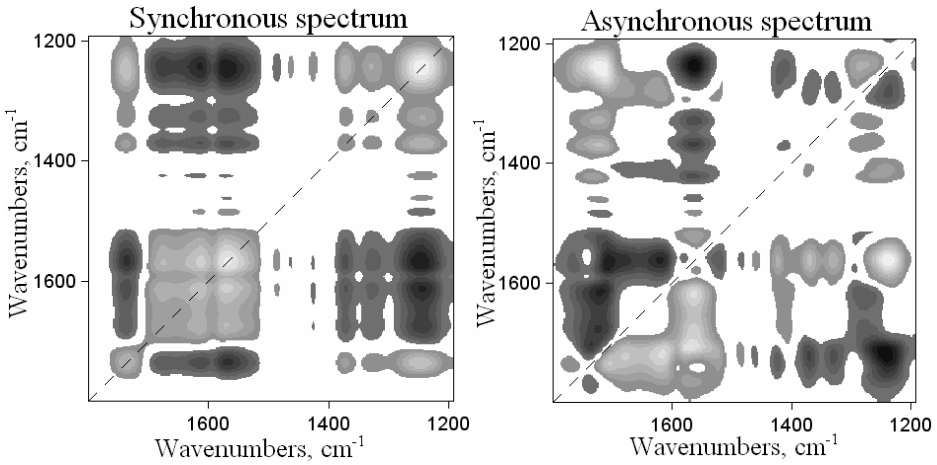

Fig. 8. Synchronous (a) and asynchronous (b) 2D-correlation spectra in the 1800–1195 cm^{-1} region issued from the exposure time-dependent IR spectra.
Biodegradation with *C. globosum*, time range of 0–70 days.

In the correlation maps two speciffic paterns were observed: the first one in the 1780–1700 cm^{-1} region, which represents the intensity and width decreases of the 1738 cm^{-1} band, and the second one, evidenced in the 1300–1200 cm^{-1} region, implying the variation of the band at 1246 cm^{-1}. The intensity and width of this band increases and, at the same time, the maximum is shifted to higher wavenumbers.

The asynchronous 2D correlation spectrum in the time range of 0–70 days (Fig. 8b) shows nine bands at 1738, 1674, 1603, 1575, 1462, 1429, 1373, 1327 and 1246 cm^{-1}. Positive cross-peaks at $\Psi(1738, 1462) > 0$, $\Psi(1738, 1429) > 0$, $\Psi(1738, 1373) > 0$, $\Psi(1738, 1327) > 0$, $\Psi(1738, 1246) > 0$, and negative cross-peaks at $\Psi(1738, 1674) < 0$, $\Psi(1738, 1603) < 0$, $\Psi(1738, 1575) < 0$, $\Psi(1603, 1575) < 0$, $\Psi(1575, 1462) < 0$, $\Psi(1575, 1429) < 0$, $\Psi(1575, 1373) < 0$, $\Psi(1575, 1327) < 0$, $\Psi(1575, 1246) < 0$, $\Psi(1429, 1373) < 0$, $\Psi(1429, 1246) < 0$ were identified. Based on the fundamental rule of an asynchronous spectrum, the spectral intensity change at 1738 cm^{-1} occurs before those at 1674, 1603, 1575, 1462, 1429, 1373, 1327 and 1246 cm^{-1}. Thus, the following sequence of spectral intensity changes was obtained:

$$1738>1575>1246>1373>1327>1462,1429>1674>1603\ cm^{-1}$$

This sequence means that the moment of the C=O of acetyl and carbonyl groups (hemicelluloses) is changing first, followed by those of conjugated C–O linkages in guaiacyl aromatic methoxyl groups and acetyl groups in xyloglucan, C–H linkages in lignin and carbohydrates, and C=C bonds of substituted aromatic ring (lignin).

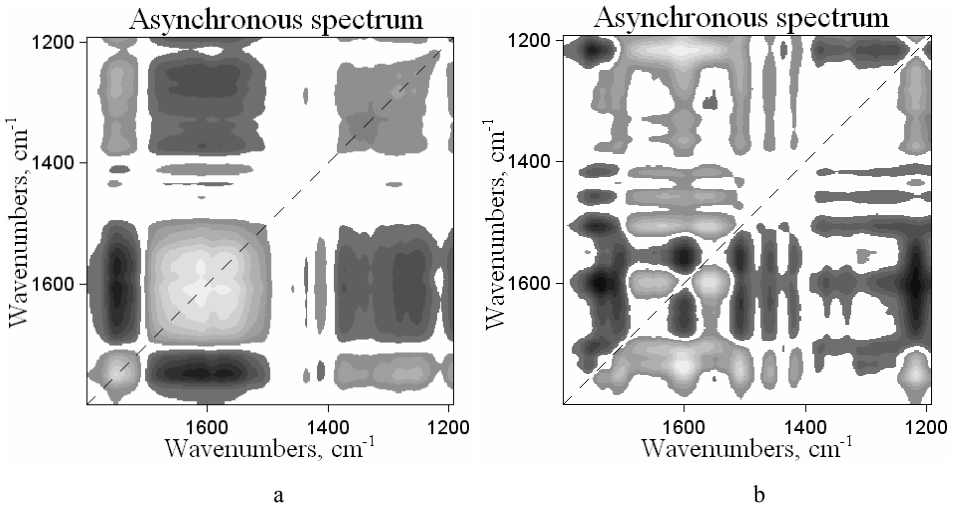

Fig. 9. Synchronous (a) and asynchronous (b) 2D-correlation spectra in the 1800–1195 cm^{-1} region issued from the exposure time-dependent IR spectra.
Biodegradation with *C. globosum*, time range of 70–133 days.

In the synchronous 2D correlation IR spectrum of the second exposure time range of 70–133 days (Fig. 9a), five auto-peaks at $\Phi(1753, 1753) > 0$, $\Phi(1598, 1598) > 0$, $\Phi(1369, 1369) > 0$, $\Phi(1284, 1284) > 0$, and $\Phi(1254, 1254) > 0$, and the corresponding positive and negative cross-peaks were identified.

At the same time, in the asynchronous 2D correlation spectrum (Fig. 9b) ten bands at 1753, 1662, 1598, 1456, 1423, 1369, 1334, 1284, 1254, and 1217 cm^{-1} were observed. Based on the fundamental rule of an asynchronous spectrum, the following sequence of spectral intensity changes was obtained:

$$1217>1254>1753>1284>1334>1369>1456,1423>1662>1598\ cm^{-1}$$

This means that the moment of the C−O−C linkages of the pyranose ring are changing first, followed by the C–O linkages in guaiacyl aromatic methoxyl groups and acetyl groups in xyloglucan, C=O linkages of carboxyl and acetyl groups in hemicelluloses (xyloglucan), C–H linkages in lignin and carbohydrates, and C=C bonds of substituted aromatic ring (lignin).

These fungi are able to use extracellular reactive oxygen species (ROS) to degrade lignocellulose materials [5]. Thus, •OH radicals can abstracts hydrogen atoms from the sugar subunits of polysaccharides (cellulose) with high rate constants. These reactions produce transient carbon-centred radicals that react rapidly with O_2 and give ROO• species. If the peroxyl radical already has a hydroxyl group on the same carbon atom, •OOH radicals will be eliminated. In the absence of α-hydroxyl group, it will undergo a variety of oxidoreductions, which can result in the cleavage of the polysaccharide chain. The modification of the IR bands with increasing the time of exposure to the fungus is due to this process.

Generally, soft-rot fungi decay is characterized by attacking wood under moist conditions, being followed by the softening of the woody tissue. Particularly, *C. globosum* is characterized by the specific action on carboxyl and acetyl groups in hemicelluloses. This fungus attacks actively cellulose and hemicelluloses, and was observed to cause the depletion of lignin in beech wood [38]. For lime wood the same behavior as suggested before was observed (demethoxylation by decreasing the bands assigned to different vibrations of methoxyl groups in lignin).

Photodegradation of lime wood (UV light, temperature, humidity)

Lime wood blocks were exposed to artificial light from a mercury lamp ($200<\lambda<700$ nm, incident light intensity 39 mW/cm^2) at a temperature of 40 ^oC and 65% relative humidity in a commercial chamber (Angelantoni CH250 Ind. Italy). The samples were removed from the chamber at regular intervals ranging from 0 up to 600 hours; the modifications were analyzed and compared to non-irradiated (reference) sample [30].

The FT-IR and 2D IR correlation spectra of photodegraded lime wood show that lignin is the most sensitive component to the degradation process, as indicated by the considerable decreases in the intensities of the characteristic aromatic lignin peak at 1505 cm^{-1} and other associated bands. The most significant differences were evidenced in the fingerprint region of 1850–1200 cm^{-1}, and thus the 2D IR correlation maps were plotted only in this region.

In the synchronous 2D correlation spectrum (Fig. 10a) eight auto-peaks at $\Phi(1785, 1785) > 0$, $\Phi(1711, 1711) > 0$, $\Phi(1649, 1649) > 0$, $\Phi(1591, 1591) > 0$, $\Phi(1502, 1502) > 0$, $\Phi(1462, 1462) > 0$, $\Phi(1423, 1423) > 0$ and $\Phi(1228, 1228) > 0$ and the corresponding positive and negative cross-peaks were observed, implying that the bands at 1785, 1711, 1649, 1591, 1502, 1462, 1423 and 1228 cm^{-1} vary during this exposure time. The different patterns which were discussed in the data simulation part can be found in these spectra. For example, the pattern which is in the 1820–1660 cm^{-1} region can be assigned to three bands which vary in the same direction (in this case, increasing).

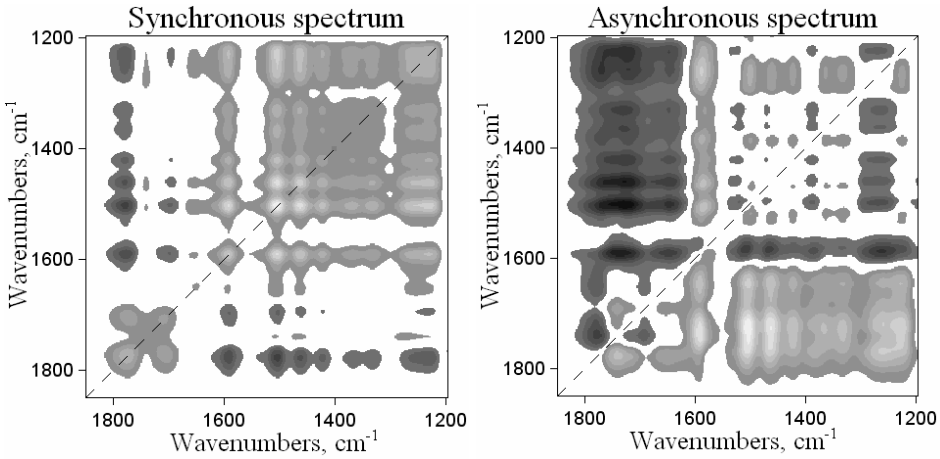

Fig. 10. Synchronous (a) and asynchronous (b) 2D-correlation spectra in the 1850–1195 cm^{-1} region issued from the exposure time-dependent IR spectra. Photodegradation time up to 600h.

The asynchronous 2D correlation spectrum (Fig. 10b) shows twelve bands at 1785, 1743, 1711, 1649, 1597, 1502, 1462, 1423, 1386, 1327, 1257 and 1228 cm^{-1}. Positive cross-peaks at $\Psi(1743, 1649) > 0$, $\Psi(1597, 1502) > 0$, $\Psi(1597, 1462) > 0$, $\Psi(1597, 1386) > 0$, $\Psi(1597, 1327) > 0$, $\Psi(1597, 1257) > 0$, $\Psi(1502, 1462) > 0$, $\Psi(1502, 1386) > 0$, $\Psi(1502, 1257) > 0$, $\Psi(1462, 1386) > 0$, $\Psi(1462, 1257) > 0$, $\Psi(1423, 1386) > 0$, $\Psi(1423, 1257) > 0$, $\Psi(1327, 1257) > 0$ and negative cross-peaks at $\Psi(1785, 1743) < 0$, $\Psi(1743, 1597) < 0$, $\Psi(1743, 1502) < 0$, $\Psi(1743, 1462) < 0$, $\Psi(1743, 1423) < 0$, $\Psi(1743, 1386) < 0$, $\Psi(1743, 1327) < 0$, $\Psi(1743, 1257) < 0$, $\Psi(1743, 1228) < 0$, $\Psi(1649, 1597) < 0$, $\Psi(1649, 1502) < 0$, $\Psi(1649, 1462) < 0$, $\Psi(1649, 1423) < 0$, $\Psi(1649, 1386) < 0$, $\Psi(1649, 1327) < 0$, $\Psi(1649, 1257) < 0$, $\Psi(1649, 1228) < 0$, $\Psi(1386, 1327) < 0$, $\Psi(1386, 1228) < 0$, $\Psi(1257, 1228) < 0$ were identified. Based on the fundamental rule of an asynchronous spectrum, the spectral intensity change at 1743 cm^{-1} occurs first and the following sequence of the spectral intensity changes was obtained:

1743>1711>1785>1597>1502>1462,1423>1327>1228>1257>1386>1649 cm^{-1}

This sequence means that the moment of C=O linkages of carboxyl and acetyl groups, non-conjugated ketones and lactones is changing first, followed by the C=C linkages of aromatic skeletal (lignin), C–H linkages in lignin and carbohydrates, C–O linkages in guaiacyl aromatic methoxyl groups, absorbed O–H and conjugated C–O in quinones. Therefore, oxidation occurs during the initial stage in hemicelluloses and then in lignin.

The bands at 1785, 1743, and 1711 cm^{-1} increase with increasing the exposure time, suggesting the formation of the carbonyl groups. This phenomenon corresponds well with lignin degradation, indicating a close relationship between them, but comparing the rate of carbonyl formation and lignin decay can be clearly observed that the former is remarkably higher than the latter. This indicates the formation of carbonyl bands which can result not only from lignin oxidation but also from other different reactions.

Many researchers have reported the reaction pathway of lignin, which starts by the photoexcitation of the aromatic carbonyl groups. The authors suggested the abstraction of hydrogen by the excited α-carbonyl group, which implies the formation of the intermediate guaiacyl and benzyl alcohol radicals. Also, the demethylation of guaiacyl radicals forms o-quinoid chromophores via several pathways [16]. Depending on *o*- or *p*-methoxy groups, the formed phenoxy radicals produce *o*- and *p*-quinones.

Quinine formation is combined with the decay of aromatic structures (loss of the skeletal vibration at 1502 and 1591 cm^{-1}) and the formation of conjugated carbonyl groups (increase of the carbonyl absorption at 1743 cm^{-1}).

Lignin degradation and carbohydrate loss as a consequence of UV irradiation of wood pulp were also shown by Kimura et al. [13, 14]. They demonstrated that the degradation of the lignin is combined with the formation of aliphatic carbonyl groups. The behavior evidenced by Kimura et al. in wood pulp is in agreement with our results in wood.

As a consequence, the formation of the aliphatic carbonyl bands in the 1800–1700 cm^{-1} region probably results from different reactions, all of them possible if free radicals are formed and induce the auto-oxidation of $–CH_2–$ or –CH(OH)– groups.

Based on the present data, the C=O groups from hemicelluloses and the free phenolic radicals in lignin were the most sensitive groups to UV irradiation.

5. CONCLUSIONS

2D FT-IR spectroscopy can be used to:

– enhance the spectral resolution by spreading spectral peaks over the second dimension, effectively resolving the overlapping of the spectral bands

– perform a detailed investigation of intra- and intermolecular interactions through the analysis of bands correlation

– investigate the chemical reactions or the kinetics of molecular vibrations by probing the specific order of spectral intensity changes

– assign the bands through correlation analysis between various bands

– correlate two different types of spectroscopy, such as Raman and IR spectroscopy

– explore the structural changes appearing once biodegradation and photo-degradation start in lime wood samples.

Acknowledgement: This paper was supported by the project PERFORM-ERA "Postdoctoral Performance for Integration in the European Research Area" (ID-57649), financed by the European Social Fund and the Romanian Government.

REFERENCES

1. BARATIERI M., BAGGIO P., FIORI L., GRIGIANTE M., *Biomass as an energy source: Thermodynamic constraints on the performance of the conversion process*, Biores. Technol., 2008, **99**, 7063-7073.
2. CONRAD M.P.C., SMITH G.D., FERNLUND G., *Fracture of Solid Wood: A Review of Structure and Properties at Different Length Scales*,Wood Fiber Sci., 2003, **35**, 570-584.
3. FEIST W.C., HON D.N.S., *The Chemistry of Solid Wood*, American Chemical Society, Washington, 1984.
4. FERRAZ A., BAEZA J., DURÁNT N., *Softwood biodegradation by an ascomycete* Chrysonilia sitophila *(TFB 27441 strain)*, Lett. Appl. Microbiol., 1991, **13**, 82-86.
5. HAMMEL K.E., KAPICH A.N., JENSEN Jr. K.A., RYAN Z.C., *Reactive oxygen species as agents of wood decay by fungi*, Enzyme Microb. Techonol., 2000, **30**, 445–453.
6. HINTERSTOISSER B., SALMÉN L., *Two-dimensional step-scan FTIR: a tool to unravel the OH-valency-range of the spectrum of Cellulose I*, Cellulose, 1999, **6**, 251–263.
7. HISHIKAWA Y., INOUE S., MAGOSHI J., KONDO T., *Novel Tool for Characterization of Noncrystalline Regions in Cellulose: A FTIR Deuteration Monitoring and Generalized Two-Dimensional Correlation Spectroscopy*, Biomacromolecules, 2005, **6**, 2468–2473.
8. HON D.N.S., SHIRAISHI N., *Wood and Cellulosic Chemistry*, Marcel Decker Inc., New York, 1991.
9. HUANG A., WANG G., ZHOU Q., LIU J., SUN S., *Study of thermal perturbation of natural bamboo fiber by two dimensional correlation analysis and fourier transform infrared spectroscopy*, Guangpuxue Yu Guangpu Fenxi (Spectrosc. Spectral Anal.), 2008, **28**, 1237–1241.
10. HUANG A.M., ZHOU Q, FEI B.H., SUN S.Q., *Study of the Eucalyptus and Poplar by generalized two-dimensional infrared correlation spectroscopy*, Guang Pu Xue Yu Guang Pu Fen Xi., 2008, **28**, 1749–1752
11. HUANG A., ZHOU Q., LIU J., FEI B., SUN S., *Distinction of three wood species by Fourier transform infrared spectroscopy and two-dimensional correlation IR spectroscopy*, J. Mol. Struct., 2008, **883–884**, 160–166.
12. JI H., KIM S.B., NODA I., JUNG Y.M., *Details of thermal behavior of spin-coated film of biodegradable poly(3-hydroxybutyrate-co-3-hydroxyhexanoate) copolymer studied by principal component analysis-based two-dimensional (PCA2D) correlation spectroscopy*, Spectrochim. Acta Part A, 2009, **71**, 1873–1876.

13. KIMURA F., KIMURA T., GRAY D.G., FT-IR *Study of UV-Irradiated Stoneground Wood Pulp*, Holzforschung, 1992, **46**, 529– 532.
14. KIMURA F., KIMURA T., GRAY D.G., FT-IR *Study of the Effect of Irradiation Wavelength on the Colour Reversion of Thermomechanical Pulps*, Holzforschung, 1994, **48**, 343– 348.
15. LABBÉ N., ANDRÉ N., RIALS T.G., KELLEY S.S., *Two-dimensional homo- and hetero-correlation technique applied to NIR and py-MBMS spectra of wood*, Holzforschung, 2008, **62**, 176-182.
16. LEARY G.J., *Photochemical Production of Quinoid Structures in Wood*, Nature, 1968, **217**, 672–673.
17. LI Y., SUN S., ZHOU Q., QIN Z., TAO J., WANG J., FANG X., *Identification of American ginseng from different regions using FT-IR and two-dimensional correlation IR spectroscopy*, Vibr. Spectrosc., 2004, **36**, 227–232.
18. LU G., ZHOU Q, SUN S, LEUNG K.S., ZHANG H., ZHAO Z., *Differentiation of Asian ginseng, American ginseng and Notoginseng by Fourier transform infrared spectroscopy combined with two-dimensional correlation infrared spectroscopy*, J. Mol. Struct., 2008, **883–884**, 91–98.
19. MA S., FREEDMAN T.B., CAO X., NAFIE L.A., *Two-dimensional vibrational circular dichroism correlation spectroscopy: pH-induced spectral changes in l-alanine*, J. Mol. Struct., 2006, **799**, 226–238.
20. NODA I., *Two-dimensional infrared (2-D IR) spectroscopy: theory and applications*, Appl. Spectrosc., 1990, **44**, 550–561.
21. NODA I., *Generalized two-dimensional correlation method applicable to infrared, Raman and other types of spectroscopy*, Appl. Spectrosc., 1993, **47**, 1329–1336.
22. NODA I., *Determination of Two-Dimensional Correlation Spectra Using the Hilbert Transform*, Appl. Spectrosc., 2000, **54**, 994–999.
23. NODA I., OZAKI Y., *Two-Dimensional Correlation Spectroscopy – Applications in Vibrational and Optical Spectroscopy*, John Wiley & Sons Ltd., Chichester, England, 2004.
24. PÉREZ J., MUÑOZ-DORADO J., de la RUBIA T., MARTÍNEZ J., *Biodegradation and biological treatments of cellulose, hemicelluloses and lignin: An overview*, Int. Microbiol., 2002, **5**, 53–63.
25. PI F., SHINZAWA H., CZARNECKI M.A., IWAHASHI M., SUZUKI M., OZAKI Y., *Self-assembling of oleic acid (cis-9-octadecenoic acid) and linoleic acid (cis-9, cis-12-octadecadienoic acid) in ethanol studied by time-dependent attenuated total reflectance (ATR) infrared (IR) and two-dimensional (2D) correlation spectroscopy*, J. Molec. Struct., 2010, **974**, 40–45.
26. POPESCU C.–M., SAKATA Y., POPESCU M.–C., OSAKA A., VASILE C., *Degradation of lime wood painting supports*, e-PRESERVATIONScience, 2005, **2**, 19–29.
27. POPESCU C.–M., POPESCU M.–C., SINGUREL G., VASILE C., ARGYROPOULOS D.S., WILLFOR S., *Spectral Characterization of Eucalyptus Wood*, Appl. Spectrosc., 2007, **61**, 1168–1177.
28. POPESCU C.–M., POPESCU M.–C., VASILE C., *Structural changes in biodegraded lime wood*, Carbohydr. Polym., 2010, **79**, 362–372.
29. POPESCU C.–M., POPESCU M.–C., VASILE C., *Characterization of Fungal Degraded Lime Wood by FT-IR and 2D IR Correlation Spectroscopy*, Microchem. J., 2010, **95**, 377–387.
30. POPESCU C.–M., POPESCU M.–C., VASILE C., *Structural analysis of photodegraded lime wood by means of FT-IR and 2D IR correlation spectroscopy*, Int. J. Biol. Macromol., 2011, **48**, 667–675.
31. POPESCU M.–C., FILIP D., VASILE C., CRUZ C., RUEFF J. M., MARCOS M., SERRANO J.L., SINGUREL GH., *Characterization by Fourier Transform Infrared Spectroscopy (FT-IR) and 2D IR Correlation Spectroscopy of PAMAM Dendrimer*, J. Phys. Chem. B, 2006, **110**, 14198–14211.
32. POPESCU M.–C., VASILE C., SINGUREL GH., *2D IR correlation spectroscopy in polymer studies*, in *New Trends in Natural and Synthetic Polymer Science*, Nova Science Publishers, 2007.

33. POPESCU M.–C., VASILE C., *Two-dimensional infrared correlation spectroscopic studies of polymer blends: conformational changes and specific interactions in polytetrahydrofuran / cholesteryl palmitate blends*, J. Optoel. Adv. Mat., 2008, **10**, 3091–3100.
34. POPESCU M.–C., VASILE C., *Melting behavior of polytetra hydrofuran/cholesteryl palmitate blends investigated by two-dimensional infrared correlation spectroscopy*, Soft Mater., 2010, **8**, 386–406.
35. POPESCU M.–C., VASILE C., CRACIUNESCU O., *Structural analysis of some soluble elastins by means of FT-IR and 2D IR correlation spectroscopy*, Biopolymers, 2010, **93**, 1072–1084.
36. POPESCU M.–C., VASILE C., *Two-dimensional infrared correlation spectroscopic studies of polymer blends – Specific interactions in polyetylene adipate/cholesteryl palmitate blends*, Spectrochim. Acta, Part A: Molec. Biomolec. Spec., 2011, **79**, 45–50.
37. QI J., HUANG K., GAO X., LI H., LIU S., ZHAO Y., XU Y., WUA J., NODA I., *Orthogonal sample design scheme for two-dimensional synchronous spectroscopy: Application in probing lanthanide ions interactions with organic ligands in solution mixtures*, J. Mol. Struct., 2008, **883–884**, 116–123.
38. SAVORY J.G., PINION L.C., *Chemical Aspects of Decay of Beech Wood by Chaetomium globosum*, Holzforschung,1958, **12**, 99-103
39. SCHMIDT O., CZESCHLIK D., *Wood and tree fungi: Biology, damage, protection, and use*, Springer, 2006.
40. SHINZAWA H., MORITA S., AWA K., OKADA M., NODA I., OZAKI Y., SATO H., *Multiple Perturbation Two-Dimensional Correlation Analysis of Cellulose by Attenuated Total Reflection Infrared Spectroscopy*, Appl. Spectrosc., 2009, **63**, 501-506.
41. SHKROB I.A., DEPEW M.C., WAN J.K.S., *Free Radical Induced Oxidation of Alkoxyphenols: Some Insights Into the Processes of Photoyellowing of Papers*, Res. Chem. Intermed., 1992, **17**, 271–285.
42. SMELLER L., HEREMANS K., *2D FT-IR spectroscopy analysis of the pressure-induced changes in proteins*, Vib. Spectrosc., 1999, **19**, 375–378.
43. STEVANIC J.S., SALMEN L., *The primary cell wall studied by dynamic 2D FT-IR interacton among components in Norway spruce (Picea abies)*, Cellulose Chem. Technol., 2006, **40**, 761–767.
44. WATANABE A., MORITA S., OZAKI Y., *Temperature-Dependent Changes in Hydrogen Bonds in Cellulose Iα Studied by Infrared Spectroscopy in Combination with Perturbation-Correlation Moving-Window Two-Dimensional Correlation Spectroscopy: Comparison with Cellulose Iβ*, Biomacromolecules, 2007, **8**, 2969–2975.
45. WATANABE S., SANO N., NODA I., OZAKI Y., *Surface Melting and Lamella Rearrangement Process in Linear Low Density Polyethylene*, J. Phys. Chem. B, 2009, **113**, 3385–3394.
46. WIEDENHOEFT A.C., MILLER R.B., *Structure and function of wood. In: R.M. Rowell, Editor, Handbook of Wood Chemistry and Wood Composites*, CRC Press, 2005.
47. YU L., XIANG B., *Two-dimensional near-infrared correlation spectroscopy study the methanol in acidic pH region*, Spectrochim. Acta, Part A: Molec. Biomolec. Spectrosc., 2008, **71**, 965–968.
48. ZHANG Y., CHEN J., LEI Y., ZHOU Q., SUN S., NODA I., *Evaluation of different grades of ginseng using Fourier-transform infrared and two-dimensional infrared correlation spectroscopy*, J. Mol. Struct., 2010, **974**, 94–102.

Received June 19, 2011